

Diffuse-reflectance spectroscopy shows a decrease in the energy of the first charge-transfer band ($t_1 \rightarrow 2e$ at $27.78 \times 10^3 \text{ cm}^{-1}$ for $\text{Cr}^{\text{VO}_4^{3-}}$ and $(\pi)t_1 \rightarrow d(e)$ (${}^1A_1 \rightarrow {}^1T_2$) at $27.03 \times 10^3 \text{ cm}^{-1}$ for $\text{Cr}^{\text{VO}_4^{2-}}$) as the valency of chromium is increased.

The absorption maxima of the octahedrally coordinated Cr^{III} ion, corresponding to the spin-allowed transitions ${}^4A_2 \rightarrow {}^4T_2$ and ${}^4A_2 \rightarrow {}^4T_1$, occur in acid solution at higher wavenumbers (17.40×10^3 and $24.40 \times 10^3 \text{ cm}^{-1}$, respectively) than in crystals of $\beta\text{-CaCr}^{\text{III}}_2\text{O}_4$ (16.12×10^3 and $21.74 \times 10^3 \text{ cm}^{-1}$, respectively).

Acknowledgment. The author has the pleasure of acknowledging the valuable assistance of Professor D. B. Russel (Professor of Chemistry at American University in Cairo, now at the University of Saskatchewan) and illuminating discussions on ESR problems. He thanks Dr. F. M. Abdul Karim (NRC) for his interest shown during the progress of IR spectroscopy and Dr. M. Z. Mostafa (NRC) for the operation of the Unicam spectrophotometer.

Registry No. $\text{Ca}_3(\text{Cr}^{\text{VO}_4})_2$, 12205-18-4; $\text{CaCr}^{\text{VI}}\text{O}_4$, 13765-19-0; $\text{CaCr}^{\text{III}}_2\text{O}_4$, 12013-31-9.

Contribution from Union Carbide Corporation, South Charleston, West Virginia 25303, and Molecular Structure Corporation, College Station, Texas 77840

[$\text{Cs}_9(18\text{-crown-6})_{14}$] $^{9+}$ [$\text{Rh}_{22}(\text{CO})_{35}\text{H}_x$] $^{5-}$ [$\text{Rh}_{22}(\text{CO})_{35}\text{H}_{x+1}$] $^{4-}$. Synthesis, Structure, and Reactivity of a Rhodium Carbonyl Cluster with Body-Centered and Cubic Arrangement of Metal Atoms

JOSÉ L. VIDAL,*^{1a} R. C. SCHOENING,^{1a} and J. M. TROUP^{1b}

Received November 9, 1979

The reaction of $\text{Rh}(\text{CO})_2\text{acac}$ with CsPhCO_2 in 18-crown-6 solvent results in the formation of high-nuclearity rhodium clusters containing 15 or more metal atoms per cluster. The isolation of [$\text{Cs}_9(18\text{-crown-6})_{14}$] $^{9+}$ [$\text{Rh}_{22}(\text{CO})_{35}\text{H}_x$] $^{5-}$ [$\text{Rh}_{22}(\text{CO})_{35}\text{H}_{x+1}$] $^{4-}$ has been carried out after 15–17 h at 150–155 °C. This cluster is the largest discrete aggregate of metal atoms reported to date. The complex has been characterized via a complete three-dimensional X-ray diffraction study. It crystallizes in the monoclinic Cm space group with $a = 76.779$ (30) Å, $b = 15.450$ (9) Å, $c = 15.741$ (5) Å, $\beta = 95.58$ (3)°, $V = 18463$ Å³, and $\rho(\text{calcd}) = 2.058 \text{ g cm}^{-3}$ for $Z = 2$. Diffraction data were collected at -110 °C with an Enraf-Nonius CAD 4 automated diffractometer and graphite-monochromatized Mo $K\alpha$ radiation. The structure was solved by direct methods and refined by difference-Fourier and least-squares techniques. All nonhydrogen atoms have been located and refined; the poor crystal properties and probably some disorder of the crown ether molecules resulted in final discrepancy indices of $R_F = 9.8\%$ and $R_{wF} = 12.2\%$ for 4390 independent reflections in the range of $0.8^\circ \leq 2\theta \leq 45^\circ$. The structures of two types of cation present in the cell, [$\text{Cs}(\text{C}_{12}\text{H}_{24}\text{O}_6)$] $^{+}$ and [$\text{Cs}_2(\text{C}_{12}\text{H}_{24}\text{O}_6)_3$] $^{2+}$, represent new species. The latter one is an unprecedented example of a "triple-decker" crown-alkali cation complex. The average cesium-oxygen bonding distances are in the ranges 3.35–3.43 Å for the former species and 3.59–4.02 Å for the latter one. The rhodium cluster consists of 12 rhodium atoms occupying the corners of two distorted rectangular prisms that share a common face. One capping atom is sitting on each of the two opposite basal faces, while six other atoms are capping three couples of vicinal prismatic faces. One of these couples is stereochemically unique, resembling the structure of $\text{M}_2(\text{CO})_8$ ($\text{M} = \text{Co}, \text{Rh}$). The two remaining rhodium atoms are encapsulated in the center of the cluster cavities. Rhodium-rhodium contacts are 2.62–3.11 and 3.41–3.87 Å for bonding and nonbonding contacts, respectively, while longer contacts of up to 4.70 Å are also present. The shortest interatomic distance of this type reported in clusters, 2.49 Å, is found between the two encapsulated atoms. There are 14 terminal, 17 edge-bridge, 2 face-bridge, and 2 semibrige carbonyls. Average distances for Rh-C and C-O are 1.81 and 1.18 Å for the first group, 2.00 and 1.19 Å for the second, 1.85, 2.15 and 1.27 Å for the third, and 1.76, 2.54 and 1.27 Å for the fourth. The anion reacts with acids and bases showing Brønsted behavior. It also reacts with carbon monoxide (1 atm, ambient temperature), probably generating two [$\text{Rh}_{15}(\text{CO})_{27}$] $^{3-}$ ions plus one [$\text{Rh}_{14}(\text{CO})_{25}\text{H}$] $^{3-}$. It is proposed the cluster could be formed by condensation of [$\text{Rh}_{15}(\text{CO})_{27}$] $^{3-}$ with [$\text{Rh}_7(\text{CO})_{16}$] $^{3-}$ or a cluster derived from it. The ^{13}C NMR spectrum of the anion shows a resonance at 211.5 ppm. The packing of rhodium atoms in the cluster corresponds to body-cubic-centered and cubic-close-packed arrangements in the outer and inner sections, respectively, with other structural characteristics indicating that the anion could model the changes expected for $\text{bcc} \rightarrow \text{ccp}$ interconversion.

Introduction

Transition metal clusters have attracted increasing attention either as potential catalysts^{1,2} or as species containing new bonding modes for organic and inorganic substrates.^{1,3} Their

role as potential useful models for a wide range of surface phenomena⁴ has also been described. In fact, clusters have been found which model the packing of atoms present in their respective metallic elements, e.g., rhodium and [$\text{Rh}_{13}(\text{CO})_{24}\text{H}_3$] $^{2-}$.⁴ Other rhodium carbonyl clusters, [$\text{Rh}_{14}(\text{CO})_{25}$] $^{4-}$ and [$\text{Rh}_{15}(\text{CO})_{27}$] $^{3-}$, have also been proposed as suitable models of the structural rearrangement occurring in some surface.⁵ A limitation of the study of cluster-surface analogies is the relatively small number of metal atoms present in a cluster^{4,6} when compared with even the smallest crystallites. Thus, a main objective in the studies of transition

- (1) (a) Union Carbide Corp. (b) Molecular Structure Corp.
- (2) (a) K. G. Caulton, M. G. Thomas, B. A. Sosinsky, and E. L. Muettterties, *Proc. Natl. Acad. Sci. U.S.A.*, **73**, 4274 (1976); E. L. Muettterties, *Bull. Soc. Chim. Belg.*, **84**, 959 (1975); G. C. Demitras and E. L. Muettterties, *J. Am. Chem. Soc.*, **99**, 2196 (1977); M. G. Thomas, B. F. Beier, and E. L. Muettterties, *ibid.*, **98**, 1296 (1976); B. F. G. Johnson, *Platinum Met. Chem. Rev.*, **22**, 47 (1978); A. K. Smith and J. M. Bassett, *J. Mol. Catal.*, **2**, 229 (1977); C. V. Pittman and R. C. Ryan, *CHEMTECH*, **170** (1978); (b) E. S. Brown, U. S. Patent 3929969 (1975); W. E. Walker, E. S. Brown, and R. L. Pruett, U. S. Patent 3878290 (1975); W. E. Walker and R. L. Pruett, 3878214 (1975); R. L. Pruett and W. E. Walker, U. S. Patent 3957857 (1976); J. L. Vidal, Z. C. Mester, and W. E. Walker, 4115428 (1978); L. A. Cosby, R. A. Fiato, and J. L. Vidal, U. S. Patent 4115433 (1978).
- (3) H. Vahrenkamp, *Struct. Bonding (Berlin)*, **32**, 1 (1977), and references therein.

- (4) E. Band and E. L. Muettterties, *Chem. Rev.*, **78**, 639 (1978); E. L. Muettterties, *Angew. Chem., Int. Ed. Engl.*, **17**, 545 (1978); E. L. Muettterties, T. N. Rhodin, E. Band, C. F. Brucker, and W. R. Pretzer, *Chem. Rev.*, **79**, 91 (1979).
- (5) S. Martinengo, G. Ciani, A. Sironi, and P. Chini, *J. Am. Chem. Soc.*, **100**, 7096 (1978).
- (6) P. Chini, *Gazz. Chim. Ital.*, **109**, 225 (1979).

metal clusters has been the preparation of complexes with a number of metal atoms approaching those in the crystallites.

Two synthetic procedures might be suitable for such preparations: redox condensation reactions under ambient conditions similar to those involved in the synthesis of known rhodium carbonyl clusters,⁷ e.g., $[\text{Rh}_{12}(\text{CO})_{30}]^{2-}$, and methods based on thermally induced growth as illustrated more recently in the preparations of $[\text{Rh}_{14}(\text{CO})_{25}]^{4-}$ and $[\text{Rh}_{15}(\text{CO})_{25}]^{3-5}$ and that of $[\text{Pt}_{19}(\text{CO})_{22}]^{4-}$, the largest transition metal carbonyl cluster described to date.⁸

We have been working during the last several years on the application of the thermal growth method to the preparation of high-nuclearity rhodium carbonyl clusters.^{9,10} This work has resulted in the synthesis of several large clusters that had been previously reported^{5,7} and in the characterization of new clusters with an unprecedentedly large number of metal atoms. This report is concerned with the synthesis, structural study, and chemical behavior of one of these species. Other similar species will be described in forthcoming publications.

Experimental Section

The materials employed in this work have been used as obtained without purification. $\text{Rh}(\text{CO})_2\text{acac}$ was obtained from Mathey-Bishop, cesium benzoate trihydrate was from Strem Chemicals, and 18-crown-6, mp 38.5–39.0 °C, was kindly prepared and supplied by Dr. Fedor Poppelsdorf of Union Carbide Corp.

Synthesis of the $[\text{Cs}(\text{18-crown-6})_n]^+$ Salt of $[\text{Rh}_{22}(\text{CO})_{35}\text{H}_x]^{(5-x)-}$. 18-Crown-6, 75 mL, was placed into a 200-mL Schlenk vessel, which was warmed to 50 °C and evacuated for several hours. A stream of carbon monoxide was then bubbled into this solvent for 0.5 h. Cesium benzoate trihydrate (0.7096 g, 2.38 mmol) was dissolved in 7.0 mL of distilled water and added to the crown, followed by the direct addition of $\text{Rh}(\text{CO})_2\text{acac}$ (3.130 g, 12.08 mmol). The system was warmed at 150–155 °C for 15–17 h under a continuous flow of gaseous carbon monoxide. The solution turned slowly from green to brown. The final dark brown solution (Figure 1a) was filtered through a fritted-disk filter warmed with steam, and a solid (3.51 g) was removed. This material was washed with 2-propanol (10 × 25 mL), vacuum dried (Figure 1b), and extracted with tetrahydrofuran (25 × 10 mL), leaving behind a residue, A (2.71 g), soluble in acetone (Figure 1c). The resulting extract was vacuum concentrated to ca. 100 mL. The slow precipitation of a solid, B, was noted under these conditions (0.31 g), and this material was used to obtain single crystals suitable for structural determination by X-ray diffraction methods (Figure 1d). The supernatant liquid was separated by filtration and treated with 2-propanol (400 mL) to form a precipitate, C (0.10 g) (Figure 1e), also recovered by filtration. The brown 18-crown-6 filtrate mentioned above was treated with a 20-fold excess of 2-propanol to precipitate a solid, D (0.80 g), which is soluble in acetone (Figure 1f). This material was used in our Brønsted acid–base experiments and in the ¹H and ¹³C NMR studies. An X-ray powder diffraction study of the solids above was conducted for comparison with those of the cesium–18-crown-6 salts of $[\text{Rh}_{15}(\text{CO})_{27}]^{3-}$ and $[\text{Rh}_{22}(\text{CO})_{35}\text{H}_{x+n}]^{(5-n)-}$, the first of which was previously characterized by us in a work to be described separately, while the latter cluster has been characterized in this work. The following results were observed:

solids	predominant cluster present	minor cluster component
A	$[\text{Rh}_{15}(\text{CO})_{27}]^{3-}$	
B	$[\text{Rh}_{15}(\text{CO})_{27}]^{3-}$	$[\text{Rh}_{22}(\text{CO})_{35}\text{H}_{x+n}]^{(5-n)-}$
C	$[\text{Rh}_{15}(\text{CO})_{27}]^{3-}$	$[\text{Rh}_{22}(\text{CO})_{35}\text{H}_{x+n}]^{(5-n)-}$
D	$[\text{Rh}_{22}(\text{CO})_{35}\text{H}_{x+n}]^{(5-n)-}$	

- (7) P. Chini, G. Longoni, and V. G. Albano, *Adv. Organomet. Chem.*, **14**, 285 (1976).
 (8) D. M. Washecheck, E. J. Wucherer, L. F. Dahl, A. Ceriotti, G. Longoni, M. Manassero, M. Sansoni, and P. Chini, *J. Am. Chem. Soc.*, **101**, 6111 (1979).
 (9) J. L. Vidal, R. A. Fiato, L. A. Cosby, and R. L. Pruett, *Inorg. Chem.*, **17**, 2574 (1978); J. L. Vidal, W. E. Walker, R. L. Pruett, and R. C. Schoening, *ibid.*, **18**, 129 (1979); J. L. Vidal and R. C. Schoening, *ibid.*, companion paper in this issue; J. L. Vidal, W. E. Walker, and R. C. Schoening, *ibid.*, companion paper in this issue.
 (10) C. H. Belin, J. D. Corbett, and A. Cisar, *J. Am. Chem. Soc.*, **99**, 7163 (1977).

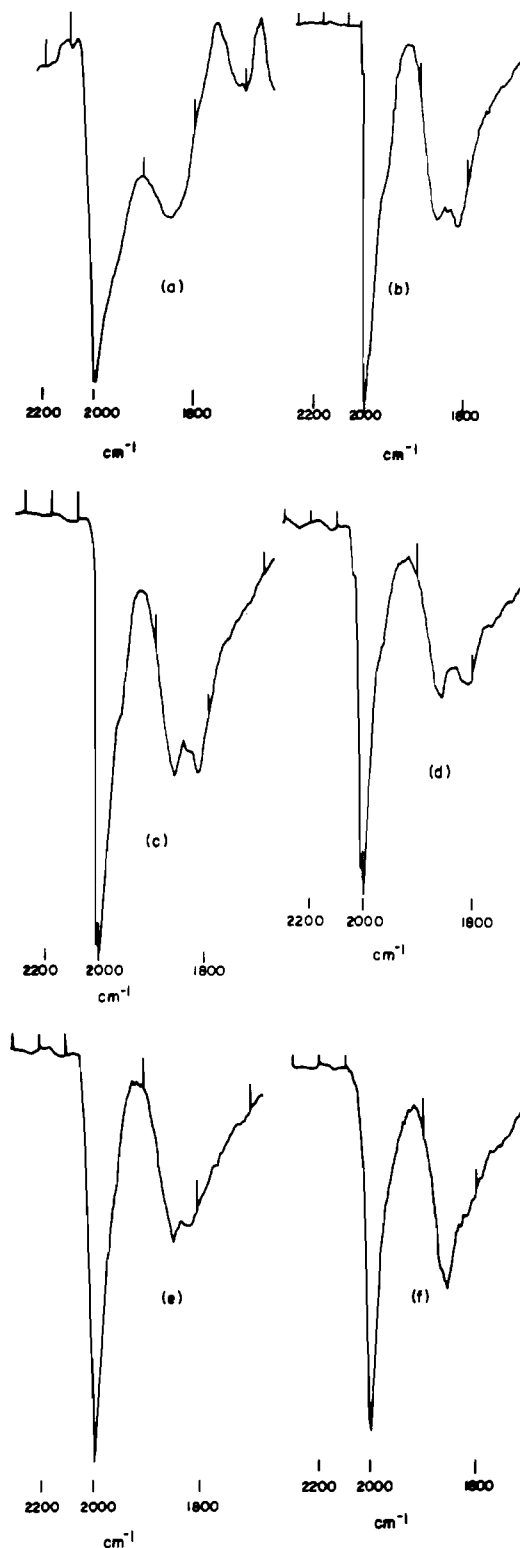


Figure 1. Infrared spectra: (a) brown 18-crown-6 filtrate; (b) crude solid product after washing with 2-propanol; (c) solids insoluble in tetrahydrofuran, A; (d) solids isolated by concentration of the tetrahydrofuran extract, from which the single crystals of $[\text{Rh}_{22}(\text{CO})_{35}\text{H}_{x+n}]^{(5-n)-}$ were obtained, B; (e) solids remaining soluble in tetrahydrofuran after precipitation with 2-propanol, C; (f) solids remaining soluble in the 18-crown-6 filtrate, D, after precipitation with 2-propanol. All the spectra were taken in acetone solutions.

All the solid products above are soluble in the usual organic polar solvents. A yield of ca. 25% of $[\text{Cs}_9(\text{C}_{12}\text{H}_{24}\text{O}_6)_{14}]^{9+}[\text{Rh}_{22}(\text{CO})_{35}\text{H}_x]^{5-}[\text{Rh}_{22}(\text{CO})_{35}\text{H}_{x+1}]^{4-}$ (solid D) was obtained based on rhodium. The elemental analysis of this product is in agreement with that expected: Anal. Calcd for $\text{C}_{476}\text{H}_{672}\text{O}_{305}\text{Rh}_{88}\text{Cs}_{18}$: C, 25.20; H,

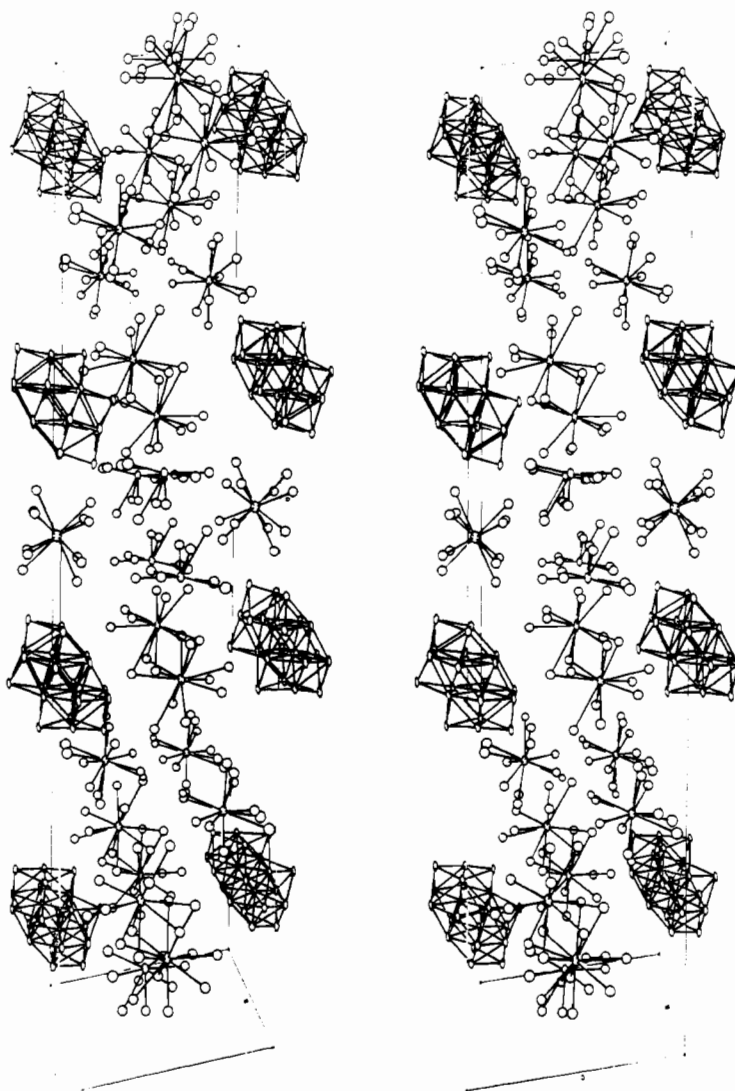


Figure 2. Stereoview of the unit cell of $[\text{Cs}_9(\text{C}_{12}\text{H}_{24}\text{O}_6)_{14}][\text{Rh}_{22}(\text{CO})_{35}\text{H}_2]^{2+}[\text{Rh}_{22}(\text{CO})_{35}\text{H}_{x+1}]^{4-}$ with the hydrogen and carbon atoms and the carbon monoxide molecules omitted.

2.96; O, 21.82; Rh, 39.57; Cs, 10.45. Found: C, 24.60; H, 2.80; O, 21.64; Rh, 39.44; Cs, 10.60.

The solid fractions A–C were dissolved together in acetone (35 mL) and precipitated with a 2-propanol solution of bis(triphenylphosphin)iminium chloride (1 g in 20 mL). The solids formed were recovered by filtration, washed with fresh 2-propanol, and dried under vacuum. This material (2.01 g) has infrared and ^{13}C NMR spectra as expected for the iminium salt of $[\text{Rh}_{15}(\text{CO})_{27}]^{2+}$.⁷ A yield for this cluster of 63.3% was obtained on the basis of rhodium.

X-ray Data Collection and Reduction. Single crystals were obtained from a solution of the above material B in acetone–18-crown-6 by vapor diffusion with isopentane.

A black prismatic crystal with dimensions $0.20 \times 0.30 \times 0.05$ mm was selected for the study. Cell constants and an orientation matrix for data collection were obtained from the least-squares refinement of the setting angles of 25 well-centered reflections. Special care was taken to ensure that no weak zones of data were missed in view of the mosaic nature of the crystals. The diffractometer, the computer, and the values of the counter aperture width, the incident-beam collimator diameter, and the crystal-to-detector distance are those used in the previous studies.⁹

Intensity data were collected via a θ – ω scan. The scan rate varied from 2 to $20^\circ/\text{min}$ in ω . The variable scan rate allows rapid data collection for intense reflections where a fast scan rate is used and ensures good counting for weak reflections where a slow scan rate is used. On the basis of a fast prescan of each reflection only those where $\sigma_I/I \leq 2.0$ are judged possible observed reflections and were

collected more slowly. This technique eliminates the lengthy data collection of unobserved reflections. The scan range was from $[2\theta(\text{Mo K}\alpha_1) - 0.8]^\circ$ to $[2\theta(\text{Mo K}\alpha_2) + 0.8]^\circ$. The advantages of the use of a variable scan rate have been already mentioned.⁹ Moving-crystal, moving-counter background counts (B_1 and B_2) were taken both at the beginning and at the end of the scan, each for half the time of the scan. Three strong representative reflections were periodically measured to check on the stability of the system. No significant changes were found. Details of the calculations of the net intensity (I) and its standard deviation (σ_I) have already been described.⁹ No evidence of extinction was observed. An absorption correction was applied to the data by using the ψ -scan technique. The total change in transmission during a typical ψ scan was 27.5%. Lorentz and polarization corrections were applied to the data.

Data were collected at room temperature (23°C) and also at -110°C . The very broad peaks observed at the former temperature were somewhat less broad at low temperature but were still not good by normal standards. The broadness of the peaks even at low temperatures indicated the possibility of disorder in the structure, although they may also originate in the loss of some solvent molecules from the cell. The low-temperature data were considered to be better and were used for the structure refinement.

Numerical information on data collection and the unit cell are given in Table I.

Solution and Refinement of the Structure. The solution of the structure with the data set collected at 23°C was obtained after more than 20 MULTAN runs with different combinations of origin reflections,

Table I. Data for the X-ray Diffraction Study of $[\text{Cs}_{4.5}(\text{C}_{12}\text{H}_{24}\text{O}_6)_7][\text{Rh}_{22}(\text{CO})_{35}\text{H}_x]$

(A) Crystal Data	
cryst system: monoclinic	
space group: $C2/m$	$\beta = 98.58 (3)^\circ$
$a = 76.779 (30) \text{ \AA}$	$V = 18\,463 \text{ \AA}^3$
$b = 15.450 (9) \text{ \AA}$	$T = -110 \pm 1 \text{ }^\circ\text{C}$
$c = 15.741 (5) \text{ \AA}$	$Z = 1$
	$\rho(\text{calcd}) = 2.058 \text{ g cm}^{-3}$
(B) Intensity Data	
radiation: Mo $K\alpha$ (λ 0.710 73 \AA)	
monochromator: graphite crystal, incident beam	
takeoff angle: 2.8°	
max 2θ : 45°	
min 2θ : 0.8°	
scan type: $\theta-\omega$	
scan speed: $2-20^\circ/\text{min}$ in ω	
scan range: symmetrical, $[2\theta(\text{Mo } K\alpha_1) - 0.8]^\circ$ to $[2\theta(\text{Mo } K\alpha_1) + 0.8]^\circ$	
reflectns collected: 13 942 total, 13 656 independent	
max dev of std reflectns: did not vary more than normal changes in counting statistics	
linear abs coeff: 28.23 cm^{-1} ; absorption corrections made with ψ -scan technique with a total change in transmission during a typical ψ scan of 27.5%	
$F(000)$: 10 998	

^a Cell constants were obtained by computer centering of 25 reflections, followed by least-squares refinement of the setting angles.

starting set reflections, $|E_{\text{min}}|$, space groups, and reflection scaling. The final conditions for the successful application of MULTAN were as follows: the symmetry was reduced to $P1$ from $C2/m$; all parity groups were rescaled so that the average E values were the same for each parity group; three origin-fixing reflections and five starting set reflections were chosen by hand; and 2000 relationships were used with a minimum E value of 2.55. In the final MULTAN run all phase sets had about the same figure of merit as in earlier runs. A fragment of the rhodium cluster was found in one of the 32 phase sets. This fragment, 10 atoms, was translated into the higher symmetry $C2/m$ cell and refined. The cluster was found to lie on the crystallographic mirror plane in space group $C2/m$. The difference Fourier map at this point revealed the remaining rhodium atoms and cesium atoms. Attempts to locate the carbonyl groups on the cluster were only partially successful.

A low-temperature data set was taken at $-110 \text{ }^\circ\text{C}$ to reduce vibrational problems in the structure and this allowed the location of all the carbonyl groups. Succeeding difference-Fourier synthesis then led to the location of the remaining nonhydrogen atoms. One carbonyl group (C(8)-O(8)) was found to be disordered in a 50%-50% arrangement above and below the mirror plane. Four cesium atoms were located on the mirror plane, and one cesium atom had a $2/m$ location. All of the crown ether groups were found to lie on crystallographic mirror planes. The high-temperature factors and poor bond distances and angles observed for the crown ether molecules are probably a consequence of the disorder of these molecules. This precludes us from making any comments concerning the structures of these molecules, except to describe their relative disposition around the cesium atoms and the Cs-O distances. An analysis of the distribution and populations of the cesium atoms and the crown ether molecules present in the cell shows an extremely complex situation that can be summarized as follows:

atom	site	coordinated O atoms and site symmetries
Cs(1)	m	O(22)[m] + O(23) + O(24) + O(25)[m] + O(26) + O(27) + O(28)
Cs(2)	m	O(29)[m] + O(30) + O(31) + O(32)[m]
Cs(3), Cs(4)	m	O(33)[m] + O(34) + O(35) + O(36)[m] + O(37)[m] + O(38) + O(39) + O(40)[m] + O(41)[m] + O(42) + O(43) + O(44)[m]
Cs(5)	$2/m$	O(45)[m] + O(46) + O(47) + O(48)[m]

Only 4390 reflections with $|F_o|^2 > 3\sigma_{|F_o|^2}$ were used in subsequent analysis. Refinement of the positional and anisotropic thermal parameters for all nonhydrogen atoms led to convergence with $R_F = 9.8\%$ and $R_{wF} = 12.2\%$. For the 130 atoms studied, the number of

variable parameters considered was 557. The esd of an observation of unit weight was then 2.76, while the maximum parameter shift was less than 1 times its esd on the cluster atoms and less than 2 times its esd on crown atoms. Additional full matrix least-squares refinement only led to oscillations in the crown ether atomic positions. Exhaustive refinement attempts of the structure in space groups Cm and $C2$ gave no improvement in the atomic positions of the disordered crown ethers and eventually led to divergence.

The function $\sum w(|F_o| - |F_c|)^2$ showed no unusual trends or appreciable dependence upon $\lambda^{-1} \sin \theta$ or upon $|F_o|$. The final difference Fourier map showed no residual electron density as high as the carbon atoms in crown ethers on a previous difference Fourier map that had a maximum peak height of $3 \text{ e } \text{ \AA}^{-3}$. In an attempt to resolve the question of a 0.5 charge on the cluster a search in the final difference Fourier map for possible H_3O^+ or other groups on $2/m$ sites in the structure showed very little electron density in these locations. Therefore, the final ratio of cluster to cations in the cell seems to be 1 cluster to 4.5 cesium atoms. Thus, the final stoichiometry of the structure is constant with $[\text{Cs}_9(\text{C}_{12}\text{H}_{24}\text{O}_6)_{14}][\text{Rh}_{22}(\text{CO})_{35}\text{H}_x]^{5-}[\text{Rh}_{22}(\text{CO})_{35}\text{H}_{x+1}]^{4-}$.

Positional parameters are included in Table II. Complete tables of observed and calculated structure factor amplitudes, thermal parameters, and bond lengths and bond angles are available as supplementary material.

Results and Discussion

The presence of 4 clusters and 18 cations in the unit cell results in an overall fractional charge for the anion of 4.5. This obvious inconvenience was recognized early in the study and resulted in an unsuccessful search for species such as organic anions or hydronium ion that might indicate an integral charge for the anion. Our inability to find such species in the positions of the final Fourier map which would correct the value of the charge (i.e., the $2/m$ sites) resulted in the assumption that two oxidation states of the anion are present in the crystal. The presence in the same cell of two similar clusters that differ in their degree of reduction has a precedent in the characterization of Ge_9^{2-} and Ge_9^{4-} . The counterion also consisted in this case of an alkali cation coordinated to a bulky cyclic-ether ligand [cryptand(2.2.2)-K]⁺.¹⁰ Since the presence of families of high-nuclearity rhodium carbonyl clusters that differ only in the number of hydrides is well-known, e.g., $[\text{Rh}_{13}(\text{CO})_{24}\text{H}_x]^{(5-x)-}$ ($x = 3, 2, 1, 0$)¹¹ and $[\text{Rh}_{14}(\text{CO})_{25}\text{H}_x]^{(4-x)-}$ ($x = 1$),^{12a-c} it appeared to us that the presence of hydrides could be responsible for the above results. In that case, the clusters present in our case could be $[\text{Rh}_{22}(\text{CO})_{35}\text{H}_x]^{5-}$ and $[\text{Rh}_{22}(\text{CO})_{35}\text{H}_{x+1}]^{4-}$. This possibility was tested by studying the proton NMR spectrum of a solution of the material in acetone- d_6 .¹³ The appearance of a weak resonance barely above the noise at $\tau = 29.5$ ppm upfield from tetramethylsilane

- (11) V. G. Albano, A. Ceriotti, P. Chini, G. Ciani, S. Martinengo and W. M. Anker, *J. Chem. Soc., Chem. Commun.*, 859 (1975); *J. Chem. Soc., Dalton Trans.*, 978 (1979).
- (12) (a) P. Chini (personal communication) et al. have suggested that $[\text{Rh}_{15}(\text{CO})_{27}]^{3-}$ could have a ^{13}C NMR spectrum with two multiplets at 216.5 and 210.5 ppm with a doublet at 182.4 ppm. (b) P. Chini (personal communication) et al. have studied the reaction of $[\text{Rh}_{14}(\text{CO})_{25}]^{4-}$ with Brønsted acids and they isolated and characterized $[\text{Rh}_{14}(\text{CO})_{25}\text{H}]^{3-}$. (c) We have studied the same reaction using ^{13}C NMR to find that two distinct species are generated upon addition of nonoxidant acids to $[\text{Rh}_{14}(\text{CO})_{25}]^{4-}$ as indicated by the independent appearance and interconversion of resonances at 212.0 and 210.0 ppm; a complete report of these results is in preparation. (d) The ratios of the multiplets resulting from the reaction of $[\text{Rh}_{22}(\text{CO})_{35}\text{H}_x]^{4.5-}$ with CO could thus be consistent with partial reaction of the initial product to generate $[\text{Rh}_{15}(\text{CO})_{25}]^{4-}$ and $[\text{Rh}_{14}(\text{CO})_{25}\text{H}_x]^{(4-x)-}$ as suggested if the assignments of the bonds at 212.0, 216.5, and 210.5 ppm to the three previous clusters is considered respectively.
- (13) A saturated solution in acetone- d_6 was placed into a 12-mm NMR tube and studied by ^1H NMR between -85 and $+40 \text{ }^\circ\text{C}$ with tetramethylsilane as external standard. The low solubility of the product at low temperatures precluded us from obtaining unequivocal spectral data under these conditions. A broad, weak resonance was detected at $40 \text{ }^\circ\text{C}$.

Table II. Final Positional Parameters with Esd's for $[\text{Cs}(\text{C}_{12}\text{H}_{24}\text{O}_6)_{1.55}]_{4.5}[\text{Rh}_{22}(\text{CO})_{35}\text{H}_x]$

atom	x	y	z	atom	x	y	z
Cs(1)	0.23162 (8)	0.0000 (0)	0.2503 (3)	O(47)	-0.0114 (10)	0.185 (5)	0.145 (5)
Cs(2)	0.04804 (9)	0.5000 (0)	0.5405 (3)	O(48)	-0.0284 (23)	0.000 (0)	0.165 (11)
Cs(3)	0.10445 (9)	0.0000 (0)	0.5065 (3)	C(1)	0.3701 (6)	0.214 (4)	1.067 (3)
Cs(4)	0.16351 (8)	0.0000 (0)	0.6297 (3)	C(2)	0.3654 (9)	0.299 (5)	0.879 (4)
Cs(5)	0.00000 (0)	0.0000 (0)	0.0000 (0)	C(3)	0.4041 (10)	0.279 (6)	0.984 (5)
Rh(1)	0.36443 (8)	0.0000 (0)	0.9349 (3)	C(4)	0.3588 (8)	0.113 (4)	1.171 (4)
Rh(2)	0.39402 (9)	0.0000 (0)	1.0249 (3)	C(5)	0.3088 (10)	0.000 (0)	0.692 (5)
Rh(3)	0.32492 (9)	0.0000 (0)	0.8032 (4)	C(6)	0.3291 (8)	0.000 (0)	1.202 (4)
Rh(4)	0.43509 (10)	0.0000 (0)	1.1433 (4)	C(7)	0.3694 (8)	0.000 (0)	1.318 (4)
Rh(5)	0.33740 (9)	0.0000 (0)	1.0960 (3)	C(8) ^a	0.4588 (9)	0.030 (5)	0.152 (4)
Rh(6)	0.38092 (9)	0.0000 (0)	1.2290 (4)	C(9)	0.5586 (10)	0.163 (6)	0.970 (5)
Rh(7)	0.36843 (5)	0.0947 (3)	1.0776 (2)	C(10)	0.3421 (8)	0.146 (4)	0.709 (4)
Rh(8)	0.40562 (6)	0.0932 (3)	1.1610 (2)	C(11)	0.3379 (6)	0.226 (3)	0.946 (3)
Rh(9)	0.42163 (6)	0.0899 (4)	0.9907 (2)	C(12)	0.4065 (6)	0.215 (3)	1.153 (3)
Rh(10)	0.39097 (6)	0.0907 (3)	0.8734 (2)	C(13)	0.3142 (6)	0.102 (3)	0.860 (3)
Rh(11)	0.35653 (6)	0.0907 (3)	0.7894 (3)	C(14)	0.3210 (6)	0.099 (3)	1.046 (3)
Rh(12)	0.33642 (6)	0.0932 (3)	0.9483 (2)	C(15)	0.3950 (7)	0.098 (4)	1.265 (3)
Rh(13)	0.36352 (6)	0.1951 (3)	0.9306 (2)	C(16)	0.4286 (9)	0.102 (5)	1.217 (4)
Rh(14)	0.39508 (6)	0.1943 (3)	1.0271 (2)	C(17)	0.4361 (17)	0.000 (0)	0.939 (8)
O(1)	0.3653 (5)	0.284 (2)	1.100 (2)	C(18)	0.4140 (7)	0.147 (4)	0.884 (3)
O(2)	0.3661 (5)	0.362 (3)	0.837 (2)	C(19)	0.4005 (10)	0.000 (0)	0.800 (5)
O(3)	0.4078 (6)	0.359 (3)	0.965 (3)	C(20)	0.3773 (9)	0.156 (5)	0.771 (4)
O(4)	0.3530 (5)	0.164 (3)	1.223 (2)	C(21)	0.3580 (9)	0.000 (0)	0.700 (4)
O(5)	0.2971 (8)	0.000 (0)	0.634 (4)	C(22)	0.1840 (6)	-0.080 (3)	0.209 (3)
O(6)	0.3232 (8)	0.000 (0)	1.269 (4)	C(23)	0.1898 (8)	-0.155 (4)	0.259 (4)
O(7)	0.3625 (9)	0.000 (0)	1.378 (4)	C(24)	0.2129 (7)	-0.230 (4)	0.334 (3)
O(8) ^a	0.4747 (8)	0.028 (5)	0.155 (4)	C(25)	0.2319 (9)	-0.230 (5)	0.347 (4)
O(9)	0.4529 (8)	0.201 (4)	1.056 (4)	C(26)	0.2564 (7)	-0.157 (4)	0.427 (3)
O(10)	0.3311 (5)	0.192 (3)	0.661 (2)	C(27)	0.2612 (6)	-0.079 (3)	0.485 (3)
O(11)	0.3297 (4)	0.285 (2)	0.949 (2)	C(28)	0.2167 (10)	-0.190 (5)	0.071 (4)
O(12)	0.4108 (4)	0.281 (2)	1.187 (2)	C(29)	0.2317 (10)	-0.229 (5)	0.085 (4)
O(13)	0.3004 (4)	0.135 (2)	0.849 (2)	C(30)	0.2618 (12)	-0.197 (6)	0.152 (5)
O(14)	0.3095 (4)	0.133 (2)	1.061 (2)	C(31)	0.2723 (10)	-0.142 (6)	0.173 (5)
O(15)	0.3992 (6)	0.138 (3)	1.338 (3)	C(32)	0.2843 (11)	-0.051 (6)	0.263 (5)
O(16)	0.4392 (6)	0.133 (3)	1.280 (3)	C(33)	0.2149 (9)	0.034 (5)	-0.013 (4)
O(17)	0.4476 (8)	0.000 (0)	0.898 (4)	C(34)	0.0529 (8)	0.415 (5)	0.315 (4)
O(18)	0.4209 (5)	0.196 (3)	0.833 (2)	C(35)	0.0413 (10)	0.342 (6)	0.327 (5)
O(19)	0.4068 (5)	0.000 (0)	0.735 (2)	C(36)	0.0296 (10)	0.272 (6)	0.452 (5)
O(20)	0.3831 (5)	0.202 (3)	0.715 (2)	C(37)	0.0286 (11)	0.265 (6)	0.546 (5)
O(21)	0.3577 (7)	0.000 (0)	0.626 (3)	C(38)	0.0148 (9)	0.344 (5)	0.641 (4)
O(22)	0.1877 (6)	0.000 (0)	0.252 (3)	C(39)	0.0103 (9)	0.443 (4)	0.645 (4)
O(23)	0.2075 (5)	-0.167 (3)	0.281 (2)	C(40)	0.1165 (7)	0.058 (4)	0.750 (3)
O(24)	0.2389 (5)	-0.164 (2)	0.408 (2)	C(41)	0.1281 (9)	0.169 (5)	0.710 (4)
O(25)	0.2549 (6)	0.000 (0)	0.440 (3)	C(42)	0.1343 (12)	0.222 (6)	0.607 (5)
O(26)	0.2132 (6)	-0.086 (3)	0.055 (3)	C(43)	0.1381 (12)	0.192 (7)	0.556 (6)
O(27)	0.2422 (9)	-0.212 (5)	0.156 (4)	C(44)	0.1446 (14)	0.069 (7)	0.416 (7)
O(28)	0.2699 (7)	-0.075 (4)	0.219 (3)	C(45)	0.1499 (16)	0.110 (8)	0.386 (7)
O(29)	0.0428 (7)	0.500 (0)	0.335 (3)	C(46)	0.0857 (20)	-0.055 (10)	0.280 (9)
O(30)	0.0413 (6)	0.337 (3)	0.426 (3)	C(47)	0.0934 (10)	-0.125 (5)	0.274 (5)
O(31)	0.0212 (7)	0.347 (4)	0.556 (3)	C(48)	0.0853 (18)	0.213 (10)	0.397 (9)
O(32)	0.0096 (25)	0.500 (0)	0.656 (12)	C(49)	0.0802 (11)	0.224 (6)	0.470 (5)
O(33)	0.1269 (14)	0.000 (0)	0.722 (7)	C(50)	0.0756 (11)	0.171 (6)	0.605 (5)
O(34)	0.1244 (13)	0.133 (7)	0.653 (6)	C(51)	0.0671 (13)	0.115 (7)	0.637 (6)
O(35)	0.1431 (10)	0.168 (5)	0.475 (5)	C(52)	0.1941 (14)	0.067 (7)	0.510 (7)
O(36)	0.1492 (11)	0.000 (0)	0.377 (5)	C(53)	0.2003 (12)	0.122 (6)	0.551 (6)
O(37)	0.0989 (13)	0.000 (0)	0.272 (6)	C(54)	0.1895 (10)	0.186 (5)	0.693 (5)
O(38)	0.0881 (11)	-0.162 (6)	0.359 (5)	C(55)	0.1847 (12)	0.220 (7)	0.742 (6)
O(39)	0.0735 (11)	0.163 (6)	0.524 (5)	C(56)	0.1750 (14)	0.097 (7)	0.829 (7)
O(40)	0.0732 (19)	0.000 (0)	0.661 (9)	C(57)	0.1704 (12)	0.038 (6)	0.874 (6)
O(41)	0.2088 (13)	0.000 (0)	0.496 (6)	C(58)	0.0435 (11)	0.084 (6)	0.117 (5)
O(42)	0.1962 (13)	0.208 (7)	0.620 (6)	C(59)	0.0430 (16)	0.141 (9)	0.103 (7)
O(43)	0.1757 (13)	0.163 (7)	0.805 (6)	C(60)	0.0150 (16)	0.208 (8)	0.157 (7)
O(44)	0.1586 (14)	0.000 (0)	0.874 (7)	C(61)	0.0063 (17)	0.208 (9)	0.118 (8)
O(45)	0.0481 (18)	0.000 (0)	0.102 (8)	C(62)	-0.0228 (18)	0.171 (10)	0.171 (8)
O(46)	0.0266 (12)	0.173 (7)	0.111 (6)	C(63)	-0.0360 (13)	-0.110 (7)	0.168 (6)

^a The weight of the parameters of these two atoms is 0.5.

and the Brønsted chemistry found for the cluster (vide infra) strongly suggest the existence of a family of compounds based on the 22 rhodium atom cluster described in this work, as is the case with the trideca- and tetradecarhodium clusters mentioned above. We have isolated one other 22 rhodium atom cluster and its structure is under study to attempt to establish this point. These results will be reported separately.

The difference of one unit in the oxidation state of a cluster

of the size and complexity of $[\text{Rh}_{22}(\text{CO})_{35}\text{H}_{x+n}]^{(5-n)-}$ should not result in appreciable differences in the interatomic distances of the two probable anions as indicated by the minor differences found for most of the structural parameters of two less complex clusters such as $[\text{Rh}_{13}(\text{CO})_{24}\text{H}_3]^{2-}$ and $[\text{Rh}_{13}(\text{CO})_{24}\text{H}_2]^{3-}$.¹¹ For this reason, we believe the structural data below are representative of the structure of the tetra- and pentaanions of $[\text{Rh}_{22}(\text{CO})_{35}\text{H}_{x+n}]^{(5-n)-}$.

Description of the Structure

The solid-state structure of the salt has been found to have two novel structural features. In addition to the characterization of a new rhodium carbonyl cluster, we have been able to characterize a new and previously uncharacterized type of alkali cation-crown ether complex. We therefore discuss these two structures separately.

Structure of the Cation. Crown ethers have been shown to coordinate with alkali cations forming 1:1 and 2:1 ligand to cation complexes depending upon the ratio of the radii of the cation and the cavity of the crown.¹⁴ The latter type of complex has been reported in several instances (e.g., [K-(benzo-10-crown-5)]⁺ and [Cs(dibenzo-18-crown-6)]⁺-SCN^{15a,b}) and has been referred to as a "sandwich" complex.^{14a} In the original publication concerning alkali cation-crown ether complexes^{14a} it was also proposed, on the basis of analytical results, that there existed "club sandwich" complexes or species containing a linear arrangement of three crown and two cation moieties with one of the crowns placed between the two alkali ions.^{14a} Structural studies reported to date^{15a} indicated instead the formation of complexes containing two alkali cations, two crown ethers, and two coordinated bridging anions, [Cs(18-crown-6)NCS]₂.^{15c}

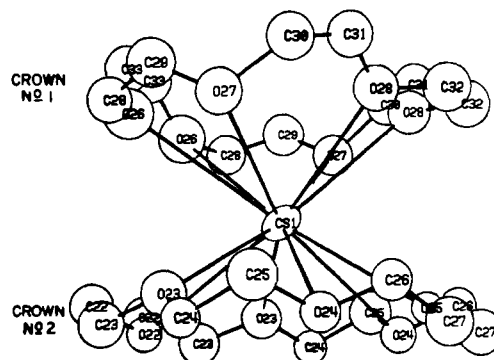
The overall composition of the cesium-crown cationic complex [Cs₉(18-crown-6)₁₄]⁹⁺ can be broken down to the three types of complexes shown here:

	[Cs(18-crown-6) ₂] ⁺	[Cs(18-crown-6)] ⁺	[Cs ₂ (18-crown-6) ₃] ²⁺
Ce atoms forming each complex	Cs(1) and Cs(5)	Cs(2)	Cs(3), Cs(4)
no. of moieties in unit cell	6	4	4

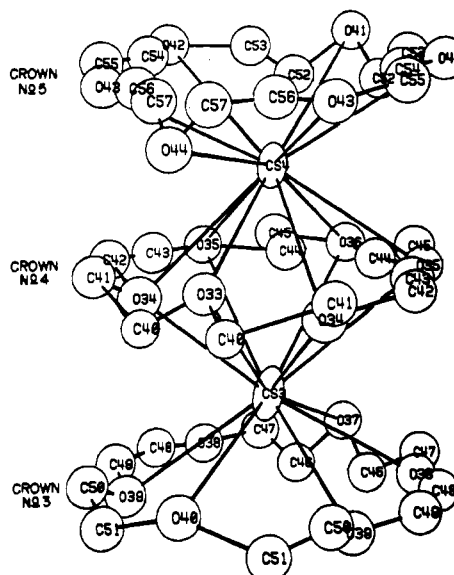
We can succinctly describe the structures of two of the new cations, [Cs(18-crown-6)]⁺ and [Cs₂(18-crown-6)₃]²⁺ (Figure 3). The former species is one more example of the already known type of sandwich complex. In contrast, the latter is an unprecedented species and it is the first characterized example of the club sandwich complex between crown ethers and alkali cations.

The large thermal factors obtained for the atoms in these two cationic complexes (Table II) probably result from disorder in the crown ether molecules, as has been previously found with other cesium-crown ether complexes.¹⁵ These results preclude any discussion concerning the relative positions of the atoms in these complexes other than the cesium-oxygen distances and the distribution of the oxygen atoms around the cations.

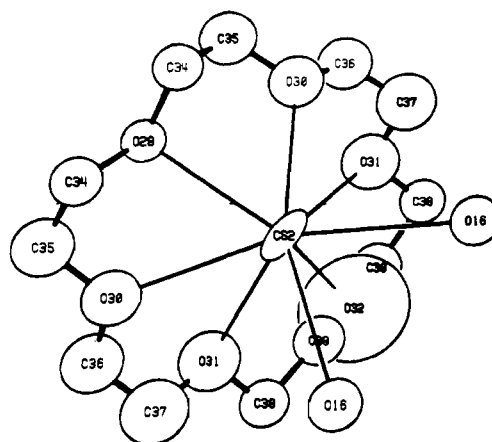
The sandwich complex [Cs(C₁₂H₂₄O₆)₂]⁺ has 12 oxygen atoms surrounding the cation and forming a hexagonal antiprism. Our results indicate that Cs(1) is located at similar distances from the oxygen atoms in both crown ether molecules as indicated by average cesium-oxygen contacts of 3.35 and



(a)



(b)



(c)

Figure 3. ORTEP diagrams of (a) [Cs(C₁₂H₂₄O₆)₂]⁺, (b) [Cs₂(C₁₂H₂₄O₆)₃]²⁺, and (c) [Cs(C₁₂H₂₄O₆)CO(16)]⁺.

3.43 Å for crown (1) and crown (2), respectively (Table III). Similar interatomic distances between these two atoms have been observed in the two related species [Cs(dibenzo-18-crown-6)NCS] and [Cs(dibenzo-18-crown-6)]⁺, 3.12–3.24 Å.¹⁵

The club sandwich complex [Cs₂(C₁₂H₂₄O₆)₃]²⁺ has 18 oxygen atoms forming a hexagonal prism. Average cesium-oxygen contacts in this case are as follows: Cs(3)-oxygen

(14) (a) C. J. Pedersen, *J. Am. Chem. Soc.*, **92**, 386 (1970); (b) J. M. Lehn, *Struct. Bonding (Berlin)*, **16**, 1 (1973).

(15) (a) M. R. Truter, *Struct. Bonding (Berlin)*, **16**, 71 (1973); (b) A. J. Layton, P. R. Mallinson, D. G. Parson, and M. R. Truter, *J. Chem. Soc., Chem. Commun.*, 694 (1973); D. G. Parsons, *J. Chem. Soc., Perkin Trans. 1*, 245 (1975); P. R. Mallinson, *J. Chem. Soc., Perkin Trans. 2*, 261 (1975); (c) M. Dobler and R. P. Phizackerley, *Acta Crystallogr., Sect. B*, **B30**, 2748 (1974); J. D. Dunitz, M. Dobler, P. Seiler, and R. P. Phizackerley, *ibid.*, **B30**, 2733 (1974); J. N. Cawse, U. S. Patent 4013700 (1977); L. Kaplan, U. S. Patent 3944588 (1976); J. N. Cawse and J. L. Vidal, U. S. Patent 4111975 (1978); Kaplan, U. S. Patent 4162261 (1979); (d) W. F. Edgell et al., *J. Am. Chem. Soc.*, **93**, 6403 (1971); **96**, 415 (1974); C. M. Lukehart, G. Paull Torrence, and J. V. Zeile, *ibid.*, **97**, 6905 (1977); D. P. Graddon, I. K. Gregor, and I. A. Siddigi, *J. Organomet. Chem.*, **102**, 321 (1975); C. D. Pribula and T. L. Brown, *ibid.*, **71**, 415 (1974); K. H. Pannell and D. Jackson, *J. Am. Chem. Soc.*, **98**, 4443 (1976); (e) D. F. Shriver and A. Alich, *Coord. Chem. Rev.*, **8**, 15 (1972), and references therein.

Table III. Interatomic Distances (Å) and Estimated Esd's for $[\text{Rh}_{22}(\text{CO})_{35}\text{H}_x]^{4-5-}$, $[\text{Cs}(\text{C}_{12}\text{H}_{24}\text{O}_6)_2]^+$, and $[\text{Cs}_2(\text{C}_{12}\text{H}_{24}\text{O}_6)_3]^{2+}$

(a) Distances for Rhodium-Rhodium			
Shorter Contacts			
Rh(1)-Rh(2)	2.492 (6)	Rh(7)-Rh(8)	2.926 (6)
Rh(1)-Rh(7)	2.660 (4)	Rh(7)-Rh(12)	2.948 (4)
Rh(1)-Rh(10)	2.764 (5)	Rh(7)-Rh(13)	2.764 (4)
Rh(1)-Rh(11)	2.676 (4)	Rh(7)-Rh(14)	2.770 (4)
Rh(1)-Rh(12)	2.622 (5)	Rh(8)-Rh(8)	2.881 (7)
Rh(1)-Rh(13)	3.015 (3)	Rh(8)-Rh(9)	3.111 (4)
Rh(2)-Rh(7)	2.679 (5)	Rh(8)-Rh(14)	2.651 (4)
Rh(2)-Rh(8)	2.625 (4)	Rh(9)-Rh(9)	2.777 (7)
Rh(2)-Rh(9)	2.655 (5)	Rh(9)-Rh(10)	2.767 (4)
Rh(2)-Rh(10)	2.745 (4)	Rh(9)-Rh(14)	2.726 (5)
Rh(2)-Rh(14)	3.003 (3)	Rh(10)-Rh(10)	2.801 (6)
Rh(3)-Rh(11)	2.839 (5)	Rh(10)-Rh(11)	2.774 (4)
Rh(3)-Rh(12)	2.732 (4)	Rh(10)-Rh(13)	2.902 (4)
Rh(4)-Rh(8)	2.732 (4)	Rh(10)-Rh(14)	2.879 (4)
Rh(4)-Rh(9)	2.833 (5)	Rh(11)-Rh(11)	2.803 (6)
Rh(5)-Rh(7)	2.847 (5)	Rh(11)-Rh(12)	3.128 (3)
Rh(5)-Rh(12)	2.727 (4)	Rh(11)-Rh(13)	2.733 (4)
Rh(6)-Rh(7)	2.838 (4)	Rh(12)-Rh(12)	2.881 (6)
Rh(6)-Rh(8)	2.724 (5)	Rh(12)-Rh(13)	2.655 (4)
Rh(7)-Rh(7)	2.926 (6)	Rh(13)-Rh(14)	2.661 (4)
Longer Contacts			
Rh(1)-Rh(3)	3.409 (6)	Rh(7)-Rh(9)	4.497 (4)
Rh(1)-Rh(5)	3.508 (5)	Rh(7)-Rh(10)	3.872 (3)
Rh(1)-Rh(14)	3.954 (4)	Rh(7)-Rh(11)	4.492 (3)
Rh(2)-Rh(4)	3.416 (6)	Rh(7)-Rh(12)	4.138 (4)
Rh(2)-Rh(6)	3.508 (5)	Rh(8)-Rh(9)	4.205 (4)
Rh(2)-Rh(13)	3.966 (4)	Rh(8)-Rh(10)	4.499 (3)
Rh(3)-Rh(13)	4.485 (4)	Rh(9)-Rh(10)	3.929 (4)
Rh(4)-Rh(14)	4.486 (5)	Rh(10)-Rh(11)	3.943 (4)
Rh(5)-Rh(6)	3.669 (6)	Rh(11)-Rh(12)	4.226 (4)
Rh(7)-Rh(8)	4.146 (4)		
(b) Rhodium-Carbonyl Bond Lengths			
Terminal Carbonyls			
Rh(3)-C(5)	1.98 (5)	Rh(11)-C(10)	1.78 (4)
Rh(5)-C(6)	1.87 (4)	Rh(13)-C(2)	1.67 (3)
Rh(6)-C(7)	1.77 (4)		
Edge-Bridge Carbonyls			
Rh(3)-C(13)	2.04 (3)	Rh(10)-C(19)	2.02 (4)
Rh(4)-C(16)	2.06 (5)	Rh(10)-C(20)	2.05 (5)
Rh(5)-C(14)	2.06 (3)	Rh(11)-C(20)	1.94 (5)
Rh(6)-C(15)	1.90 (4)	Rh(11)-C(21)	2.00 (3)
Rh(8)-C(15)	1.94 (3)	Rh(12)-C(11)	2.05 (3)
Rh(8)-C(16)	1.86 (5)	Rh(12)-C(13)	2.04 (3)
Rh(8)-C(12)	1.89 (3)	Rh(12)-C(14)	2.08 (3)
Rh(9)-C(17)	2.03 (7)	Rh(13)-C(11)	2.07 (3)
Rh(9)-C(18)	1.92 (4)	Rh(14)-C(12)	2.08 (3)
Rh(10)-C(18)	1.96 (4)		
Semibridge and Face-Bridge Carbonyls			
Rh(5)-C(4)	2.56 (4)	Rh(7)-C(1)	1.85 (4)
Rh(6)-C(4)	2.52 (4)	Rh(13)-C(1)	2.16 (3)
Rh(7)-C(4)	1.76 (4)	Rh(14)-C(1)	2.13 (3)
(c) Carbonyl C-O Lengths			
Terminal Carbonyls			
C(5)-O(5)	1.18 (6)	C(10)-O(10)	1.26 (4)
C(6)-O(6)	1.21 (5)	C(14)-O(14)	1.08 (3)
C(7)-O(7)	1.15 (5)		
Edge-Bridge Carbonyls			
C(11)-O(11)	1.12 (3)	C(17)-O(17)	1.17 (8)
C(12)-O(12)	1.16 (4)	C(18)-O(18)	1.26 (4)
C(13)-O(13)	1.16 (3)	C(19)-O(19)	1.19 (5)
C(14)-O(14)	1.08 (3)	C(20)-O(20)	1.26 (5)
C(15)-O(15)	1.29 (4)	C(21)-O(21)	1.16 (4)
C(16)-O(16)	1.28 (5)		
Semibridge and Face-Bridge Carbonyls			
C(1)-O(1)	1.27 (4)	C(4)-O(4)	1.27 (4)
Selected Distances for the Cs-18-Crown-6 Cationic Complexes			
Cs(1)-O(22)	3.38 (3)	Cs(3)-O(38)	3.52 (8)
Cs(1)-O(23)	3.25 (3)	Cs(3)-O(39)	3.51 (8)
Cs(1)-O(24)	3.53 (3)	Cs(3)-O(40)	3.67 (8)
Cs(1)-O(25)	3.25 (3)	Cs(4)-O(33)	3.35 (8)
Cs(1)-O(26)	3.45 (3)	Cs(4)-O(34)	3.70 (8)
Cs(1)-O(27)	3.74 (3)	Cs(4)-O(35)	3.73 (8)
Cs(1)-O(28)	3.26 (3)	Cs(4)-O(36)	3.96 (8)
Cs(2)-O(29)	3.20 (3)	Cs(4)-O(41)	4.32 (8)
Cs(2)-O(30)	3.09 (3)	Cs(4)-O(42)	4.09 (8)
Cs(2)-O(31)	3.16 (4)	Cs(4)-O(43)	3.76 (8)
Cs(2)-O(32)	3.69 (2)	Cs(4)-O(44)	3.93 (8)
Cs(3)-O(33)	3.57 (8)	Cs(5)-O(45)	3.80 (8)
Cs(3)-O(34)	3.29 (8)	Cs(5)-O(46)	3.65 (8)
Cs(3)-O(35)	4.03 (8)	Cs(5)-O(47)	3.84 (8)
Cs(3)-O(36)	4.25 (8)	Cs(5)-O(48)	3.64 (8)
Cs(3)-O(37)	3.66 (8)		
(d) Cesium-CO(16) Distance			
Cs(2)-O(16)	3.51 (3)		

atoms in crown (3), 3.59 Å; Cs(3)-oxygen atoms in crown (4), 3.79 Å; Cs(4)-oxygen atoms in crown (4), 3.69 Å; Cs(4)-oxygen atoms in crown (5), 4.03 Å. These distances are longer than those previously observed in cesium complexes with ligands containing oxygen donor centers such as crowns (vide supra)¹⁵ or glymes.¹⁴ It is not possible to ascribe the causes of the elongation of the Cs(4)-crown (5) contacts to steric interactions between crown (4) and crown (5) because a similar behavior is absent from the other end of the complex. Instead, the longer Cs(4)-oxygen atom contacts in crown (5) could result from the lack of significant bonding interactions between these atoms. In spite of that, the conformation of the crown (5) molecule, its position in the cell, and the distances to other cations strongly indicate the presence of bonding interactions between those atoms. Unfortunately, the lack of other examples of complexes with a similar structure preclude further analysis in this respect.

An even more relevant complex from the point of view of cluster chemistry is perhaps $[\text{Cs}(2)(18\text{-crown-6})]^+$. The stereochemistry of this species (Figure 3) has the relative arrangement of crown and alkali cation expected from the respective radii of the crown's cavity, 1.37 Å, and the ion, 1.69 Å, as indicated by other results.¹⁴ The cesium-oxygen contacts for this species (Table III), 3.09-3.69 Å, are in the range usually observed for cesium complexes of this type (vide supra).

This cation, Cs(2), is also interacting with the two symmetry-related bridging carbonyl ligands, CO(16), of the nearest cluster anion, as indicated by a Cs(2)-O(16) distance of 3.51 Å. The coordination sphere around Cs(2) resembles that of $[\text{Cs}(18\text{-crown-6})\text{NCS}]_2$.

The $[\text{Cs}(2)(18\text{-crown-6})]^+$ structure illustrates one mode of interaction between alkali cations and cluster carbonyl complexes. Reports concerning the effect of ion pairing in the properties of catalysts used in the conversion of CO-H₂ to polyalcohols^{15c} suggest that this kind of interaction may be important. Interactions similar to that of Cs(2)-CO(16) have been observed between other alkali cations and transition-metal carbonyls, and their effects on spectroscopic or chemical behavior of these complexes have been reported.^{15d} In any case, the preference of Cs(2) for the bridging carbonyl as a coordination site may be fortuitous, but it is in agreement with previous results that have established the coordinative preference of Lewis acids for these sites in their interactions with clusters.^{16e}

Structure of the Anion. The rhodium core of the anion (Figure 4a) consists of two staggered rectangular prisms sharing one common face (Rh(7), Rh(7), Rh(10), Rh(10)) with an interstitial rhodium atom in the center of each prism (Rh(1), Rh(2)). These two atoms lie in the plane that passes through the two capping rhodium atoms (Rh(3), Rh(4)) lo-

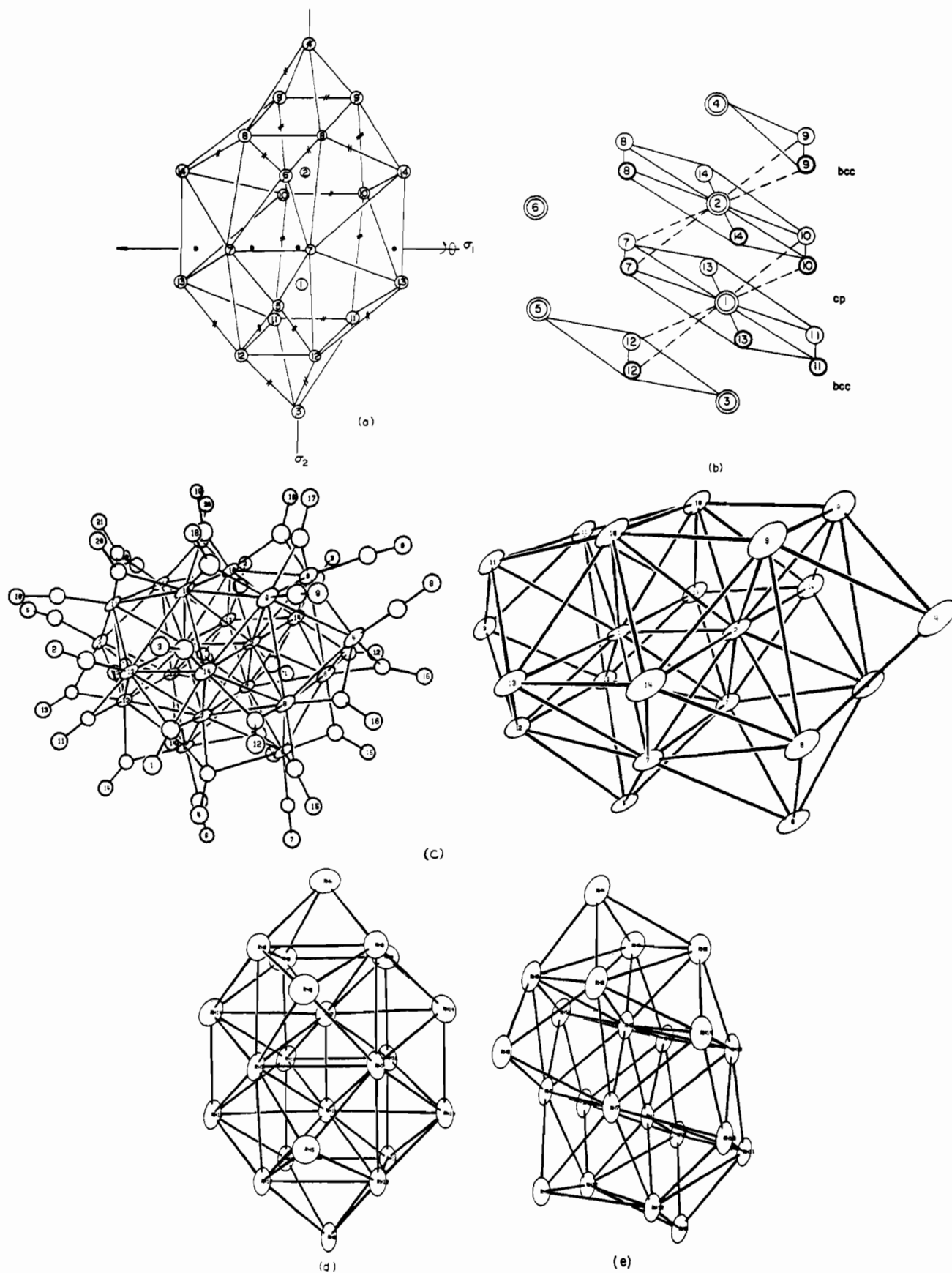


Figure 4. (a) Scheme of the structure of $[\text{Rh}_{22}(\text{CO})_{35}\text{H}_{x++}]^{(5-n)-}$ showing the positions of terminal, \odot , edge-bridge, $++$, and face-bridge or semibrige, \bullet , carbonyls. The idealized planes of symmetries σ_1 and σ_2 and the C_2 axis of symmetry are also shown. (b) Layer structure of the anion showing its cubic packing. The rhodium atoms represented by double circles are located on the σ_2 plane of symmetry, and those by single lightface and boldface circles are below and above this plane, respectively. The cp and bcc notations refer to the cubic-close-packed and body-centered-cubic arrangements of rhodium atoms in the central and outer sections. (c) ORTEP diagram of the anion with and without the carbonyls. The thermal ellipsoids enclose 20% of their electron density. (d) ORTEP diagram of the cluster corresponding to the orientation in part a. (e) ORTEP diagram of the cluster corresponding to the orientation in part b.

Table IV. Least-Squares Plane Calculations for the Rhodium Atoms Shown and Dihedral Angles between Planes

plane no.	atom	\bar{X}	\bar{Y}	\bar{Z}	dist, Å
1	Rh(2)	27.8456	0.0000	15.9518	-0.224
	Rh(8)	28.4167	1.4404	18.0712	0.138
	Rh(8')	28.4167	-1.4404	18.0712	0.138
	Rh(10)	27.9673	1.4007	13.5944	0.126
	Rh(10')	27.9673	-1.4007	13.5944	0.126
	Rh(14)	27.9218	3.0019	15.9866	-0.152
	Rh(14')	27.9218	-3.0019	15.9866	-0.152
2	Rh(1)	25.7848	0.0000	14.5513	0.069
	Rh(6)	26.3605	0.0000	19.1294	0.195
	Rh(7)	25.7571	1.4629	16.7732	-0.175
	Rh(7')	25.7571	-1.4629	16.7732	-0.175
	Rh(11)	25.5202	1.4015	12.2875	0.027
	Rh(11')	25.5202	-1.4015	12.2875	0.027
	Rh(13)	25.7249	3.0139	14.4851	0.016
Rh(13')	25.7249	-3.0139	14.4851	0.016	
3	Rh(1)	25.7848	0.0000	14.5513	-0.145
	Rh(5)	23.3316	0.0000	17.0588	0.108
	Rh(7)	25.7571	1.4629	16.7732	-0.118
	Rh(10)	27.9673	1.4007	13.5944	0.026
	Rh(11')	25.5202	-1.4015	12.2875	0.055
	Rh(12')	23.6034	-1.4406	14.7596	-0.006
	Rh(14)	27.9218	3.0019	15.9866	0.081
4	Rh(2)	27.8456	0.0000	15.9518	0.147
	Rh(6)	26.3605	0.0000	19.1294	-0.110
	Rh(7')	25.7571	-1.4629	16.7732	0.123
	Rh(8)	28.4167	1.4404	18.0712	0.006
	Rh(9)	30.0454	1.3885	15.4208	-0.056
	Rh(10)	27.9673	-1.4007	13.5944	-0.025
	Rh(13)	25.7249	-3.0139	14.4851	-0.084
plane no.	plane no.	dihedral angle, deg			
1	2	0.0			
3	4	5.6			

cated on each of the outer faces of the prisms (Rh(8), Rh(8), Rh(9), Rh(9) and Rh(11), Rh(11), Rh(12), Rh(12)). The six remaining metal atoms form three capping couples, (Rh(5), Rh(6), and two Rh(13)–Rh(14)) located on vicinal pairs of the trapezoidal faces of the prisms in such a way that the two uncapped square faces (Rh(9), Rh(9), Rh(10), Rh(10) and Rh(10), Rh(10), Rh(11), Rh(11)) are opposite the unique capping couple (Rh(5), Rh(6)). Two perpendicular planes of symmetry, σ_1 and σ_2 , contain the Rh(7)–Rh(7) and Rh(10)–Rh(10) edges and the Rh(3)–Rh(1)–Rh(2)–Rh(4) axis, respectively. They define a binary axis of symmetry perpendicular to the plane of the paper that passes through the midpoints of the Rh(7)–Rh(7) and Rh(10)–Rh(10) edges. This results in an idealized C_{2v} symmetry for the metallic cage.

Another view of the anion (Figure 4b) shows the four layers of rhodium atoms present in the anion.¹⁶ The planar arrangement of Rh(2), -(8), -(8), -(10), -(10), -(14), -(14) and Rh(1), -(6), -(7), -(7), -(11), -(11), -(13), -(13) (Figure 4b) or of Rh(1), -(5), -(7), -(10), -(11), -(12), -(14) and Rh(2), -(6), -(7), -(8), -(9), -(10), -(13) (Figure 4c) have been confirmed by least-squares plane calculations (Table IV). The relative position of these layers corresponds to that expected for a cubic close packing of hard spheres.¹⁷ In fact, the sections between the outer and inner layers have a body-centered-cubic arrangement, evident from the positions of the couples of Rh(8), Rh(9), and Rh(10) around Rh(2) and of Rh(7), Rh(11), and Rh(12) around Rh(1). These cubes are slightly distorted (vide infra). The coordination around the central rhodium atoms (Rh(1), Rh(2)) shows each of these atoms as having two short contacts to atoms in the outer layers (vide infra) and four short and two longer (Rh(1)–Rh(13) and

Rh(2)–Rh(14)) contacts to the surrounding atoms in its same hexagonal plane. This results in a four-plus-two-coordination of these atoms in the outer sections of the cluster (Figure 4b) as required for a bcc arrangement.¹⁷ In contrast, the section between the two parallel hexagonal layers has cubic close packing, ccp. The positions of Rh(1), Rh(2), Rh(9), Rh(9), Rh(10), Rh(10) and Rh(13), Rh(14) are those expected for a ccp of hard spheres although some distortion from the ideal arrangement is present. The coordination between these and surrounding atoms confirms this packing. The presence of two types of packing of rhodium atoms in a cluster has a precedent in the reported presence of hcp and bcc packings in $[\text{Rh}_{15}(\text{CO})_{27}]^{3-}$. It was suggested there⁵ that two of the bonds between the central atom and the rhodium atoms defining its surrounding hexagonal plane are longer than the others as a possible consequence of the hcp \rightarrow bcc interconversion. This analogy, together with the presence of a similar situation for the length of the rhodium–rhodium distances of Rh(1) and Rh(2) and the relative positions of their shorter and longer interatomic distances, suggests that the structure of our cluster could illustrate the changes involved in a ccp \rightarrow bcc interconversion.

The metal–metal distances of the anion vary widely (Table III). The shorter contacts on the surface of the cluster are between 2.651 and 2.945 Å (average 2.796 Å), and the longer contacts are 3.111 Å (Rh(8)–Rh(9)) and 3.128 Å (Rh(11)–Rh(12)) (average 3.119 Å) and a very long one of 3.872 Å between Rh(7) and Rh(10). These values, except for the last one, are in the range usually accepted for bonding interactions between rhodium atoms in this kind of compound,⁷ although the distance of 3.119 Å is borderline in this respect. Similar lengths have been reported for $[\text{Rh}_{14}(\text{CO})_{25}]^{4-}$,^{5,9} in a situation where they could be considered as probably corresponding to rhodium–rhodium bonding contacts.

The two distorted basal rectangular faces are of practically the same size as concluded from the lengths of their shorter (Rh(8)–Rh(8) = 2.881 Å, Rh(9)–Rh(9) = 2.777 Å, Rh(12)–Rh(12) = 2.881 Å, Rh(11)–Rh(11) = 2.803 Å) and longer edges (Rh(8)–Rh(9) = 3.111 Å, Rh(11)–Rh(12) = 3.128 Å). The difference between the lengths of the shorter, e.g., Rh(7)–Rh(7) and Rh(10)–Rh(10), and longer edges, e.g., Rh(7)–Rh(10), is larger for the face common to both halves of the cluster, 2.926 vs. 3.870 Å. These edges define two rectangular faces of equal size (Rh(7), Rh(7), Rh(12), Rh(12) and Rh(7), Rh(7), Rh(8), Rh(8)) that are capped by Rh(5) and Rh(6), respectively, and two smaller but equal square faces at the opposite side of the cluster (Rh(9), Rh(9), Rh(10), Rh(10) and Rh(10), Rh(10), Rh(11), Rh(11)). They also result in the two sets of four trapezoidal faces of equal size at both sides of the faces capped by Rh(5) and Rh(6). These faces are larger than any other face of the cluster. Another consequence of the previous distance is the bending of the cluster as indicated by average values of 162.9 and 164.9° for the Rh(8)–Rh(7)–Rh(12) and Rh(9)–Rh(10)–Rh(11) angles, respectively.

The capping atoms Rh(13) and Rh(14) are shifted ca. 0.3 Å from the centers of the trapezoidal faces and located ca. 1.56 Å above the surface of their respective faces, forming an almost linear arrangement with the encapsulated atoms as indicated by an average value of 176.5° for the Rh(13)–Rh(central)–Rh(14) angle. A linear arrangement is also formed by the two apical atoms Rh(3) and Rh(4) with the two encapsulated atoms. These two capping atoms are ca. 1.84 Å above the plane of the capped faces. A unique capping couple is that formed by Rh(5) and Rh(6). These atoms are placed ca. 2.00 Å above the faces at ca. 0.43 Å from their centers.

(16) This figure was kindly supplied to us by Professor Paolo Chini of the University of Milan, after seeing the anion's structure.

(17) A. F. Wells, "Structural Inorganic Chemistry", 3rd ed., Clarendon Press, Oxford, 1962, pp 112–144.

The interatomic distance between Rh(5) and Rh(6), 3.669 Å, is longer than the same distance between the two atoms of the other capping pairs, Rh(13)–Rh(14), 2.661 Å. This is a consequence of the bending of the edges Rh(8)–Rh(7)–Rh(12) and Rh(9)–Rh(10)–Rh(11) caused by the proximity of the two central atoms to the Rh(7)–Rh(10) plane.

The two central rhodium atoms, Rh(1) and Rh(2), are separated by 2.492 Å. This is the shortest contact reported between rhodium atoms in this kind of complex. The usual range for this contact in these species is 2.58–3.10 Å.^{7,9} Shorter rhodium–rhodium bond lengths have been found with simpler species. In fact, the shortest bond of this type, 2.386 Å, present in Rh₂(AcO)₄ has been regarded as in accord with a triple bond.¹⁸

Other interatomic distances involving these two atoms are within usual ranges, with average values for the shorter and longer distances between them and the atoms on the hexagonal layers of 2.679 and 3.012 Å, respectively. The two central atoms are not in close contact with the two apical (Rh(3), Rh(4)) and the two unique capping atoms (Rh(5), Rh(6)) as indicated by interatomic distances of 3.412 and 3.508 Å, respectively. By contrast, they are in close contact with the other four capping atoms with distances of 3.012 Å between them. Thus, the central atoms are located in the center of the two prismatic cavities. They are located at 1.450, 1.508, and 1.692 Å from the surfaces of the faces capped by Rh(13)–Rh(14), Rh(5)–Rh(6), and Rh(3)–Rh(4), respectively.

The location of the carbonyl ligands is shown in the drawing of the cluster in Figure 4a and in a more complex fashion in the scheme of Figure 4c. There are six unique terminal carbonyls bonded to Rh(3), Rh(5), Rh(11), Rh(11), Rh(13), and Rh(13) and related to those coordinated to the mirror image of these metal atoms by the plane of symmetry σ_1 . Nine edge-bridge carbonyls are found in one of the halves of the cluster with their counterparts located across the plane σ_1 . Another carbonyl of this type, CO(20) is located on the axis of symmetry. In addition, there are two face-bridge carbonyls sitting on the triangular faces defined by Rh(7)–Rh(13)–Rh(14) and two semibridge carbonyls placed between Rh(5), Rh(6), and Rh(7). These ligands sit on the plane of symmetry σ_1 .

Unfortunately, the lack of a better crystal has resulted in relatively high discrepancy indices. These do not affect in an appreciable way the positions of the heavy atoms but it could be considered as a potential limitation on the interpretation of the distances involving the carbonyl groups. Thus, the independent Rh–C and C–O distances (Table III) are accurate only to the first decimal place. In spite of that, the average rhodium–carbon distances for the terminal and edge-bridge ligands, 1.81 and 2.00 Å, respectively, are similar to those found in other compounds of this type. It is the same with the average C–O distances, 1.17 and 1.19 Å, respectively.

The edge-bridge carbonyls are symmetrical but the face-bridge carbonyls are asymmetrical. These ligands are equidistant from the two capping atoms, Rh(13) and Rh(14), and they are closer to them, 1.85 Å, than to the other rhodium atom, Rh(7), 2.15 Å. A similar situation occurs with the semibridge carbonyls¹⁹ between Rh(5), Rh(6), and Rh(7). In this case the Rh–C length involving the last atom, 1.76 Å, is that expected for a terminal ligand, while the same distance in the case of the former atoms, 2.54 Å, is longer than that for an edge- or face-bridge ligand. The severe bending of the CO ligand, 151° for the Rh(7)–C(4)–O(4) angle, corresponds to that expected for this type of ligand. The usual decrease in the C–D bond order in cases of multiple CO bridging is

shown also for these carbonyls with carbon–oxygen bond lengths of 1.27 Å for CO(1) and CO(4).

The crowding of the carbonyl ligands is especially evident in the section of the cluster around Rh(5) and Rh(6). C–C contacts of 2.51 and 2.53 Å are present between the carbon atoms of CO(1), CO(4) and CO(12), CO(16), respectively. Longer contacts of this type, 2.66 and 2.78 Å, are found between the bridge ligands CO(19), CO(17) and CO(19), CO(21). These ligands are bridging the edges of the square faces parallel to the plane of symmetry σ_1 , and their relatively short C–C nonbonding contact probably results from the back-bending deformation of the cluster skeleton and the subsequent steric interaction with the terminal carbonyls around the apical rhodium atoms. Indicative of such crowding may be the drastic bending of the terminal carbonyl ligands CO(3), CO(5), and CO(8) with Rh–C–O angles of 161, 169, and 164°, respectively. The bending of the latter two ligands located on Rh(3) and Rh(4) toward the edges Rh(9)–Rh(9) and Rh(11)–Rh(11) could result from the steric interactions with surrounding carbonyls as indicated by C–C contacts of 2.61 Å—for CO(5)–CO(13) and CO(8)–CO(16). The steric demands of these ligands in turn restrict the space available for the edge-bridge ligands C(17), C(19), and C(21), forcing them together, which results in the other edge bridges located on the same face, CO(18) and CO(20), being very far apart, at 4.51 Å. In turn, this forces a close nonbonding C–C contact between CO(18) and CO(3) which results in the bending of CO(3) away from the uncapped square faces. Other C–C nonbonding contacts are between 2.70 and 3.60 Å.

The uniqueness of the moiety formed by Rh(5), Rh(6), and the carbonyls coordinated to these atoms results not only from the lack of bonding interaction between the two capping metals previously mentioned but also from the singular ligand distribution around these atoms. There are five Rh–C bonds for each atom. Two of these bonds are to bridge carbonyls located between the two rhodium atoms. Formally, and obviously in an idealized way, the whole moiety resembles the stereochemistry of the bridge form of Co₂(CO)₈.²⁰

Reactivity

The probable existence of several species of rhodium–carbonyl–hydrido clusters of general formula [Rh₂₂(CO)₃₅H_x]^{(n-x)-} was already mentioned. The results obtained during the study of the Brønsted chemistry of our cluster are consistent with that. Infrared monitoring of the reaction of an acetone solution of the compound with increasing amounts of acids²¹ shows a stepwise increase in the frequency of the carbonyl bonds as shown below. This is consistent with the decrease in metal cage back-bonding to these ligands expected to occur upon protonation of the cluster as previously shown for [Rh₁₃(CO)₂₄H_x]^{(5-x)-}¹¹ and [Rh₁₇S₂(CO)₃₂]³⁻.⁹ These changes were reversed by addition of cesium hydroxide but other side products now under study were also generated. In contrast, the reaction of the initial cluster with cesium hydroxide²¹ resulted in a decrease in the frequency of the carbonyl absorptions as expected if an increase in the charge of the cluster has occurred. Acidification of the final solution allowed the regeneration of the initial spectrum. These changes are consistent with the presence of hydrides in the initial

(18) K. G. Caulton and F. Albert Cotton, *J. Am. Chem. Soc.*, **91**, 6517 (1969); F. Albert Cotton, *Acc. Chem. Res.*, **2**, 240 (1969).

(19) F. A. Cotton and J. M. Troup, *J. Am. Chem. Soc.*, **96**, 1233 (1974).

(20) G. G. Sumner, M. P. Klug, and L. E. Alexander, *Acta Crystallogr.*, **17**, 732 (1964).

(21) These reactions were studied by dissolving the cesium–18-crown-6 salt of the cluster in either acetone or sulfolane and adding a 2% solution of HSO₃CH₃, a nonoxidant acid, in either solvent. The changes were monitored by infrared and ¹³C NMR spectroscopy. Similar experiments were conducted with CsOH and a 0.009 M solution. These results will be reported in detail in a future publication.

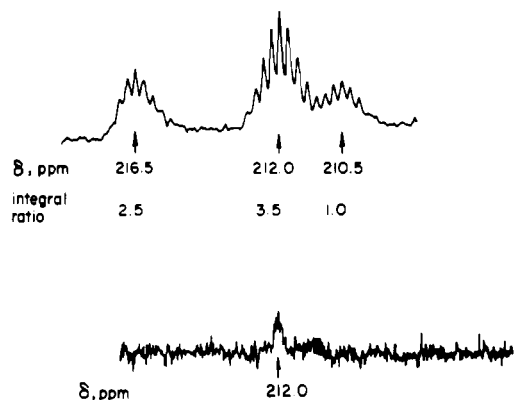
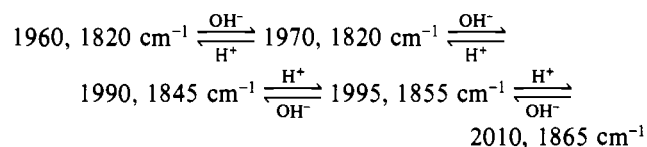


Figure 5. ^{13}C NMR spectrum of an acetone- d_6 solution of $[\text{Cs}-(\text{C}_{12}\text{H}_{24}\text{O}_6)_{1.56}]_{4.5}[\text{Rh}_{22}(\text{CO})_{35}\text{H}_x]^{3-}$: (top) before enrichment and (bottom) after enrichment with 50% ^{13}C . The chemical shifts are given with respect to tetramethylsilane.

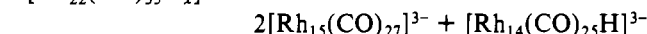
Table V. Carbonyl Distribution as a Function of Cluster Size and Surface Atoms in the Case of High-Nuclearity Rhodium Clusters

cluster	CO:Rh		CO bridge: CO terminal
	total	surface	
$[\text{Rh}_{13}(\text{CO})_{24}\text{H}_3]^{2-}$	1.85	2.00	1.00
$[\text{Rh}_{17}\text{S}_2(\text{CO})_{32}]^{3-}$	1.88	2.00	1.00
$[\text{Rh}_{15}(\text{CO})_{27}]^{3-}$	1.80	1.93	1.08
$[\text{Rh}_{14}(\text{CO})_{25}]^{4-}$	1.79	1.92	1.78
$[\text{Rh}_{22}(\text{CO})_{35}\text{H}_{x+n}]^{(5-n)-}$	1.59	1.75	1.92

clusters and we are working on the characterization of the resulting species.



The severe steric crowding by the carbonyl ligands already mentioned and the low CO:Rh ratio present in the cluster are probably responsible for its reactivity with carbon monoxide. This reaction was followed by ^{13}C NMR spectroscopy. The initial anion has a spectrum under these conditions¹³ that consists of a broad multiplet at 212.0 ppm downfield from tetramethylsilane used as external standard (Figure 5). After reaction of this solution for 24 h with 90% carbon-13 monoxide (1 atm, 30 °C) there are three multiplets in the spectrum at 216.5, 212.0, and 210.5 ppm. These results are consistent with partial fragmentation of the initial cluster to $[\text{Rh}_{15}(\text{CO})_{27}]^{3-}$ ^{12a} and $[\text{Rh}_{14}(\text{CO})_{24}\text{H}_x]^{(4-x)-}$ ($x \geq 1$).^{12b,c} The suggested assignments^{12d} are consistent with the occurrence of the reaction



Other Remarks

The infrared spectra taken to monitor the synthesis (Figure 1) could be assigned to $[\text{Rh}_{22}(\text{CO})_{35}\text{H}_{x+n}]^{(5-n)-}$ (2010, 1860, 1820 cm^{-1}) and to $[\text{Rh}_{15}(\text{CO})_{27}]^{3-}$ (1995, 1840 cm^{-1}). The infrared spectrum of the former anion is in agreement with that expected from the correlation between the position for the main terminal carbonyl absorption and the metal atom to negative charge ratio.⁷ This absorption is predicted by that correlation to occur around 2010–2015 cm^{-1} . It has been noted that the reliability of that correlation is higher when comparison is made between complexes of the same metal with similar local symmetries and ratio of bridge to terminal carbonyls.⁷ This ratio is maximum for the 22 rhodium atom species among rhodium carbonyl clusters (Table V), but the aforementioned correlation is seemingly followed in this case

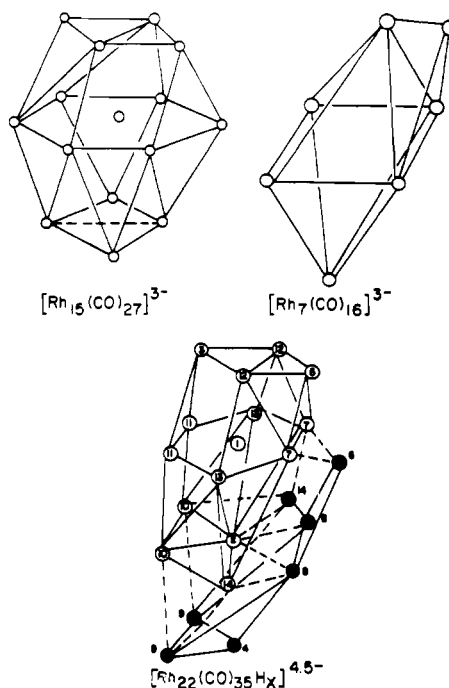


Figure 6. Arrangement of the rhodium atoms showing the probable structural relationship between the three clusters.

as well as in others for which the number of metal atoms in the clusters is unusually large, e.g., $[\text{Pt}_3(\text{CO})_6]_n^{2-}$ ($n = 5, 6$),²² although some concern has been raised in this respect.²³

$[\text{Rh}_{22}(\text{CO})_{35}\text{H}_{x+n}]^{(5-n)-}$ is the largest discrete homonuclear aggregate of metal atoms fully described to date. The maximum number of metal atoms previously reported in an aggregate of this type was 19 in the recently described structure of $[\text{Pt}_{19}(\text{CO})_{22}]^{4-}$.⁸ There are some similarities between these two clusters that could be ascribed to their large sizes. The presence of two completely encapsulated metal atoms is one. Another is the low ratios of carbon monoxide to total metal atoms and to metal atoms on the cluster's surface. Comparison of the variation of these ratios in a series of rhodium carbonyl anionic clusters shows that there is a decrease in these values upon increasing the number of metal atoms (Table V). This is probably a result of the flattening of the polyhedral surface upon increasing cluster size because the steric requirements of the carbonyls are larger when they are parallel to each other.⁶ The increase in the number of surface metal atoms that occurs with increase in cluster size is probably responsible for the bridge:terminal carbonyl ratio being maximum for the largest cluster (Table V). This could be caused by the tendency of the surface atoms to be coordinatively saturated together with the increasing carbonyl crowding expected otherwise.

The steps involved in the formation of larger clusters from lower nuclearity species are not well-known in general.⁷ It has been possible to establish that cluster growth occurs by condensation of a preformed cluster with a mononuclear species, e.g., " $\text{Rh}(\text{CO})_2^{+}$ "⁵ or $[\text{Rh}(\text{CO})_4]^-$,⁹ but there is not evidence, that we are aware of, even indirectly implying that condensation reactions between two defined clusters occur to form a larger cluster with a number of metal atoms corresponding to the sum of those in the condensing species. Of course, appropriate equations can certainly be proposed.⁷ Thus, it is important that the arrangement of metal atoms in $[\text{Rh}_{22}(\text{CO})_{35}\text{H}_{x+n}]^{(5-n)-}$, $[\text{Rh}_{15}(\text{CO})_{27}]^{3-}$, and $[\text{Rh}_7(\text{CO})_{16}]^{3-}$ (Figure

(22) G. Longoni and P. Chini, *J. Am. Chem. Soc.*, **98**, 7225 (1976).

(23) M. Primet, J. M. Bassett, E. Garbowski, and M. V. Mathieu, *J. Am. Chem. Soc.*, **97**, 3653 (1975).

6) suggests that the condensation of the two latter species could be responsible for the formation of the former one. This proposal is probably validated by the predominance of $[\text{Rh}_{15}(\text{CO})_{27}]^{3-}$ in the solid fractions above in which $[\text{Rh}_{22}(\text{CO})_{35}\text{H}_{x+n}]^{(5-n)-}$ is present. We believe that the aggregation of $[\text{Rh}_{15}(\text{CO})_{27}]^{3-}$ with $[\text{Rh}_7(\text{CO})_{16}]^{3-}$ in the presence of protons, e.g., provided by a nonoxidizing protonic acid such as trifluoromethylsulfonic, could produce the 22 rhodium atom cluster.²⁴

We are attempting to optimize the synthesis of $[\text{Rh}_{22}(\text{CO})_{35}\text{H}_{x+n}]^{(5-n)-}$, on the last hypothesis, and to obtain evidence for the processes involved in cluster growth, mainly by studying the redox reactions of high-nuclearity rhodium carbonyl clusters,^{25a} e.g., $[\text{Rh}_7(\text{CO})_{16}]^{3-}$, $[\text{Rh}_{13}(\text{CO})_{24}\text{H}_x]^{(5-x)-}$, $[\text{Rh}_{14}(\text{CO})_{25}]^{4-}$, $[\text{Rh}_{15}(\text{CO})_{27}]^{3-}$, and $[\text{Rh}_{22}(\text{CO})_{35}\text{H}_{x+n}]^{(5-n)-}$, and

the Brønsted acid-base chemistry of $[\text{Rh}_7(\text{CO})_{16}]^{3-}$ and $[\text{Rh}_{15}(\text{CO})_{27}]^{3-}$.^{25b}

Finally, it should be noted that the synthetic procedure followed for the preparation of $[\text{Rh}_{22}(\text{CO})_{35}\text{H}_{x+n}]^{(5-n)-}$ has also provided an unexpected new synthesis for $[\text{Rh}_{15}(\text{CO})_{27}]^{3-}$. This cluster can now be prepared in 63% yield by the procedure described in this work from commercially available $\text{Rh}(\text{CO})_2\text{acac}$. Nevertheless, we will report soon another synthesis that results practically in quantitative yields of $[\text{Rh}_{15}(\text{CO})_{27}]^{3-}$ with very short working time.^{25c}

Acknowledgment. The authors appreciate the authorization for publication of this work by Union Carbide Corp. and the encouragement toward applied basic research from Dr. George L. O'Connor.

Registry No. $\text{Rh}(\text{CO})_2\text{acac}$, 14874-82-9; CsPhCO_2 , 17265-04-2; $[\text{Ph}_3\text{P}=\text{NPPH}_3]_3[\text{Rh}_{15}(\text{CO})_{27}]$, 75506-17-1; Cs , 7440-46-2; 18-crown-6, 17455-13-9.

Supplementary Material Available: Complete tables of structural factors, atomic distances and angles, and positional and thermal parameters (42 pages). Ordering information is given on any current masthead page.

(24) J. L. Vidal and R. C. Schoening, submitted for publication in *J. Organomet. Chem.*

(25) (a) J. L. Vidal and R. C. Schoening, to be submitted for publication in *J. Am. Chem. Soc.*; (b) J. L. Vidal and R. C. Schoening, submitted for publication in *J. Organomet. Chem.*; (c) J. L. Vidal and R. C. Schoening, submitted for publication in *Inorg. Chem.*

Contribution from Union Carbide Corporation,
South Charleston, West Virginia 25303

$[\text{Rh}_{10}\text{P}(\text{CO})_{22}]^{3-}$. A Transition-Metal Carbonyl Cluster with a Metal Polyhedron Based on the Bicapped Square Antiprism As Illustrated by the Structural Study of the Benzyltriethylammonium Salt

JOSÉ L. VIDAL,* W. E. WALKER,[†] and R. C. SCHOENING¹

Received November 12, 1979

The reaction of $\text{Rh}(\text{CO})_2\text{acac}$ with triphenylphosphine in the presence of cesium benzoate and cesium borohydride in tetraethylene glycol dimethyl ether solution resulted in the selective formation of $[\text{Rh}_{10}\text{P}(\text{CO})_{22}]^{3-}$ (76% yield) after 4 h of contact time under 400 atm of carbon monoxide and hydrogen ($\text{CO}:\text{H}_2 = 1$) at 140–160 °C. The cluster has been isolated as the cesium and benzyltriethylammonium salts, both of which are stable to moisture and oxygen. These salts are soluble in polar organic solvents, e.g., acetone, but insoluble in solvents of lower polarity. The $[\text{C}_6\text{H}_5\text{CH}_2\text{N}(\text{C}_2\text{H}_5)_3]_3[\text{Rh}_{10}\text{P}(\text{CO})_{22}]$ complex has been characterized via a complete three-dimensional X-ray diffraction study. The complex crystallizes in the space group *Cc* with $a = 25.011$ (3) Å, $b = 16.348$ (4) Å, $c = 18.267$ (4) Å, $\alpha = \gamma = 90.0$ (1)°, $\beta = 101.47$ (1)°, $V = 7319.7$ Å³, and $\rho(\text{calcd}) = 2.045$ g cm⁻³, for a molecular weight of 2253.24 and $Z = 4$. Diffraction data were collected with an Enraf-Nonius CAD 4 automated spectrometer using graphite-monochromatized Mo K α radiation. The structure was solved by direct methods and refined by difference-Fourier and least-squares techniques. The rhodium cluster was found to have a 50:50 disorder when rotated 45° about the noncrystallographic fourfold axis in the cluster. All nonhydrogen atoms have been located and refined: final discrepancy indices are $R_F = 6.4\%$ and $R_{wF} = 7.7\%$ for 2700 reflections in the range of $0.5^\circ < 2\theta < 45^\circ$. The anion's structure shows 10 rhodium atoms on the corners of a bicapped square antiprism with the phosphorus atom placed on the center of the cluster. This is the first instance in which this polyhedron has been reported for a transition-metal cluster. Average bonding distances for the anion are in the ranges $\text{Rh-Rh} = 2.864\text{--}3.007$ Å and $\text{Rh-P} = 2.446\text{--}3.012$ Å with Rh-C and C-O distances similar to those usually observed for these complexes. ¹³C and ³¹P NMR results are interpreted as indicative of the fluxionality of the carbon monoxide and rhodium atoms cores, respectively. The reversibility of the reaction $[\text{Rh}_{10}\text{P}(\text{CO})_{22}]^{3-} + 3\text{CO} \rightleftharpoons [\text{Rh}_9\text{P}(\text{CO})_{21}]^{2-} + [\text{Rh}(\text{CO})_4]^-$ has been established under ambient- and high-pressure conditions.

Introduction

The ability of rhodium carbonyl clusters to accommodate atoms of the elements in the main groups of the periodic table was first illustrated in $[\text{Rh}_6(\text{CO})_{15}\text{C}]^{2-}$ and similar carbide species² and more recently for sulfur and phosphorus with $[\text{Rh}_{17}(\text{S})_2(\text{CO})_{32}]^{3-}$ and $[\text{Rh}_9\text{P}(\text{CO})_{21}]^{2-}$.^{3,4} These anions were found to be more stable than rhodium carbonyl clusters in which the heteroatom was absent, e.g. $\text{Rh}_6(\text{CO})_{16}$ or $[\text{Rh}_7(\text{CO})_{16}]^{3-}$, at least with respect to the transformation usually

observed for the latter type of species under high pressures of carbon monoxide and hydrogen into $[\text{Rh}_5(\text{CO})_{15}]^-$ and $[\text{Rh}(\text{CO})_4]^-$.⁵

- (1) Dr. Jan Troup of Molecular Structure Corp. conducted the structural studies reported in this work.
- (2) V. Albano, P. Chini, G. Ciani, S. Martinengo, and M. Sansoni, *J. Chem. Soc., Chem. Commun.*, 299 (1974); *J. Chem. Soc., Dalton Trans.*, 305 (1975).
- (3) J. L. Vidal, R. A. Fiato, L. A. Cosby, and R. L. Pruett, *Inorg. Chem.*, **17**, 2574 (1978).
- (4) J. L. Vidal, R. C. Schoening, R. L. Pruett, and W. E. Walker, *Inorg. Chem.*, **18**, 129 (1979).
- (5) J. L. Vidal and W. E. Walker, *Inorg. Chem.*, **19**, 896 (1980).

[†] Deceased.